

Extension of Collisionless Discharge Models for Application to Fusion-Relevant and General Plasmas

Leon Kos¹, Jože Duhovnik¹, Nikola Jelić²

¹University of Ljubljana, Faculty of Mechanical Engineering Aškerčeva 6, SI-1000 Ljubljana, Slovenia, leon.kos@lecad.fs.uni-lj.si, joze.duhovnik@lecad.fs.uni-lj.si

²Association EURATOM-ÖAW, University of Innsbruck, Department of Theoretical Physics, A-6020 Innsbruck, Austria, nikola.jelic@uibk.ac.at

ABSTRACT

Defining and finding the plasma-sheath boundary (also referred to as “plasma edge”, “sheath edge” or “sheath entrance”) is a problem of general relevance in plasma physics, and particularly so in the context of laboratory, space and fusion plasmas. In a most general approach this problem starts from the Poisson equation under the condition that (i) the electron density distribution is a known function of local potential, (ii) the ion source velocity distribution is known (iii) with additional assumption that the potential profile is monotonic. The basic unknowns of the problem to be found are the spatial potential profile and the final ion-velocity distribution. Once this solution is found, the moments of the velocity distribution, i.e. density, particle flux energy, and thermal fluxes are calculated based on the velocity distribution as calculated in any location of the system like e.g., scrape-off layer (SOL) in Tokamak devices. From a physical point of view the problem was defined by Bissell and Johnson(B&J) [Phys. Fluids **30**, 779 (1987)] as a task to find the ion potential profile and ion velocity distribution in a plane parallel discharge with a Maxwellian ion source. The B&J model is a generalization of well known Tonks-Langmuir (T&L) [Phys. Rev. **34**, 876 (1929)] discharge characterized by the so-called “cold” ion source. Unlike the T&L model, which can be readily solved analytically, attempts on solving the B&J model with a so-called “warm” ion source were done only numerically. Since the applicability of numerical solutions has been limited only to a narrow range of the ion-source temperature for many years, Kos et al. [Phys. Plasmas **26**(9), (2009)] recently tackled and solved the problem without any approximation of the integral equation kernel. The solution of Kos et al. is valid without any restriction regarding the ion temperature, i.e., applicable to both general and fusion plasmas with high ion temperatures. However, it still remains restricted to the specific case of ionization strength distribution, which is according to B&J proportional to the local electron density. In this paper we extend further the Kos et al. model to the case of constant ionization strength distribution.

1 INTRODUCTION

The Tonks-Langmuir [1] problem of collisionless discharges is a rather old and elementary one but, unfortunately, solved only under various assumptions which facilitate obtaining the solution but restricting its range of validity to particular applications. A general mathematical formulation of the problem can be expressed as a task to find function $\Psi(\Phi)$. Our mathematical formulation of the problem can be expressed in the form of a fairly general integro-differential equation

$$\varepsilon^2 n(\Phi) \frac{1}{\Psi^3} \frac{d\Psi}{d\Phi} = 1 - \lambda \int_0^\Phi \Psi(\Phi') \mathcal{K}(\tau(\Phi' - \Phi)) d\Phi' \quad (1)$$

with prescribed singular kernel \mathcal{K} , prescribed function $n(\Phi)$, arbitrary parameters ε and τ and the eigenvalue of problem λ .

Tonks and Langmuir found that the plasma and sheath problem can be split into “plasma approximation” where strict quasineutrality is assumed and “sheath approximation” with the electric field taking the role. The corresponding two regions of the plasma–wall transition layer are often referred as “the presheath” and “the Debye sheath”. They found approximate solutions for these two regions for plane, cylindrical and spherical geometries. Their “intuitive” approach of splitting the plasma-sheath equation into two parts was later rendered into a rigorous mathematical context by Caruso and Cavaliere [2], who employed for this purpose the boundary layer theory by van Dyke. This approach in plasma physics is now known as the “two-scale” approximation. Following this approach Harrison and Thompson (H&T) [3] upgraded Tonks and Langmuir approximate solution to an exact analytic one, however, holding for cold ion source distribution under the assumption of strict quasineutrality ($\varepsilon = 0$). Soon after H&T publication Self [4], however, announced a complete numerical solution, i.e., with the quasineutrality assumption removed, but still with a singular (cold) ion source ($T_n = 0$). Emmert et al. [5] tackled the plasma solution ($\varepsilon = 0$) with a regular (warm) ($T_n \neq 0$) but artificial ion source, prepared in advance to yield a Maxwellian ion distribution function. Bissell and Johnson [6], however, have decided to start from a more realistic, i.e., Maxwellian ion source, and found a numerical solution within a limited range of ion source temperatures. Their model was constrained by their choice of the kernel approximation and polynomial approximation of the model. Soon after their work Scheuer and Emmert (S&E) [7] used a better kernel approximation enabling them to find a solution also holding in the range of small ion source temperatures, but, unfortunately, not for relatively ‘warm’ ion sources, which is of high importance to fusion application. Several years after the S&E work the numerical method, libraries and computing resources dramatically increased. Kos et al. [8] recently became able to employ an exact kernel instead of an approximate one. Kos et al. solved the plasma problem with a Maxwellian source without any restriction regarding the ion temperature, however, for $\varepsilon = 0$ and for a commonly adopted assumption of the ionization source profile. Here we extend the investigations of Kos et al. to another kind of ionization profile.

2 THEORETICAL BACKGROUND

The general formulation of the problem in plane-parallel symmetric discharge consists in simultaneously solving Boltzmann’s kinetic equation for the ion velocity distribution function (VDF) $f_i(x, v)$,

$$v \frac{\partial f_i}{\partial x} - \frac{e}{m_i} \frac{d\Phi}{dx} \frac{\partial f_i}{\partial v} = S_i(x, v), \quad (2)$$

and the Poisson's equation

$$-\frac{d^2\Phi}{dx^2} = \frac{e}{\varepsilon_0}(n_i - n_e). \quad (3)$$

The source term $S_i(x, v)$ on the right-hand side of Eq. (2) describes microscopic processes assumed for a particular scenario of interest, x is the Cartesian space coordinate, v is the particle velocity, e is the positive elementary charge, m_i is the ion mass, $\Phi(x)$ the electrostatic potential at position x , ε_0 is the vacuum dielectric constant and $n_{i,e}$ are the ion and electron densities, respectively.

The schematic diagram of the geometry of the problem is shown in Fig. 1. The plates at

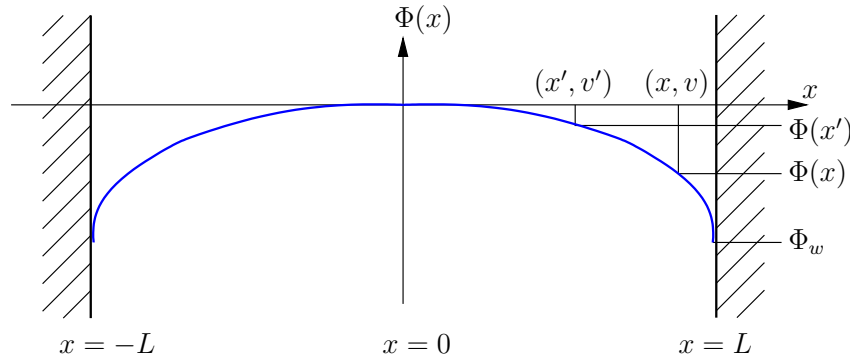


Figure 1: The geometry and coordinate system.

$x \pm L$ are assumed to be perfectly absorbing and electrically floating. The electrostatic potential $\Phi(x)$ is assumed to be monotonic decreasing (for $x > 0$) and is defined to be zero at $x = 0$. Below we give a comprehensive analysis of the Tonks-Langmuir mode starting from the general solution of kinetic Eq. (2). The source term $S_i(x, v)$ is in general

$$S_i(v, x) = Rn_n n_e(x) f_n \left(\frac{v}{v_{T_n}} \right) H \left(\frac{m_i v^2}{2} \right), \quad (4)$$

where R is the ionization rate, n_n is the density of neutrals. The electrons follow Boltzmann distribution

$$n_e(x) = n_0 \exp \left\{ \frac{e\Phi(x)}{kT_e} \right\}. \quad (5)$$

with n_0 the electron density at $x = 0$. We employ the Heaviside step function as denoted by $H(z)$ for assuring a positive sign of the kinetic energy of the ions. The velocity distribution function $f_n(v/v_{T_n})$ of the neutrals in our work is normalized as

$$\int_{-\infty}^{\infty} f_n \left(\frac{v}{v_{T_n}} \right) dv = 1, \quad (6)$$

where $v_{T_n} = \sqrt{kT_n/m_i}$ is the thermal velocity of born ions defined by temperature T_n of the neutral gas, $T_n \equiv T_{i,src}$. Due to the symmetry we further consider the right-hand half of the discharge, $x \geq 0$. For the ion flux onto the wall from Eqs. (2), (4) and (6) we find $\Gamma_i = Rn_n L n_{e,av}$, where $n_{e,av}$ represents the average value of the electron density over the system:

$$n_{e,av} = \frac{1}{L} \int_0^L n_e(x) dx. \quad (7)$$

The requirement that the ion current must be equal to the electron current at the wall enables us to write $\Gamma_i = \Gamma_e$, and

$$LRn_n n_{e,av} = \frac{1}{\sqrt{2\pi}} v_{T_e} n_0 \exp \left\{ \frac{e\Phi_w}{kT_e} \right\}, \quad (8)$$

where $v_{T_e} = \sqrt{kT_e/m_e}$, and m_e, T_e are the electron mass and temperature respectively, Φ_w is the wall potential. With the help of an auxiliary function

$$F_n \left(\frac{v}{v_{T_n}} \right) = \sqrt{2\pi} \cdot v_{T_n} f_n \left(\frac{v}{v_{T_n}} \right) \quad (9)$$

the source term (4) acquires the form

$$S_i(x, v) = \frac{1}{L} B n_e(x) F_n \left(\frac{v}{v_{T_n}} \right) H \left(\frac{m_i v^2}{2} \right), \quad (10)$$

$$B = \frac{1}{2\pi} \sqrt{\frac{T_e}{T_n} \frac{m_i}{m_e} \frac{n_0}{n_{e,av}}} \exp \left\{ \frac{e\Phi_w}{kT_e} \right\}. \quad (11)$$

with B related to the ionization frequency ν_i and the characteristic ionization length λ_i is:

$$\nu_i = B \frac{\sqrt{2\pi}}{L} v_{T_n}, \quad \text{and} \quad \lambda_i = \frac{c_s}{\nu_i} = \frac{L}{B} \sqrt{\frac{T_e}{2\pi T_n}}. \quad (12)$$

The general solution of Eq. (2) with the source term Eq. (10) is

$$f_i^\pm(x, v) = \pm \frac{B}{L} n_0 \int \frac{dx'}{\sqrt{v'^2}} \exp \left(\frac{e\Phi(x')}{kT_e} \right) F_n \left(\pm \frac{\sqrt{v'^2}}{v_{T_n}} \right) H(v'^2) + \bar{f}_i^\pm \left(v'^2 + \frac{2e}{m_i} \Phi(x') \right), \quad (13)$$

where $v'^2 = v^2 - 2e[\Phi(x') - \Phi(x)]/m_i$. In Eq. (13) f_i^\pm denotes the distribution function of the ions moving in the positive („+”) and negative („-”) directions of the x -axis. Functions $\bar{f}_i^\pm(x, v)$ are the arbitrary functions corresponding to the homogeneous part of Eq. (2) to be constrained by conditions: (a) At the center of the system, $x = 0$, the distribution function must be symmetric in the velocity space $f_i^+(0, v) = f_i^-(0, v)$. (b) Due to perfect absorption there are no ions at the wall surface, $x = L$, moving with the negative velocity (it means from the wall): $f_i^-(L, v) = 0$. After straightforward calculations we obtain the following solution of the Boltzmann kinetic equation for the arbitrary distribution function of neutrals.

$$f_i^+(x, v) = B \frac{n_0}{L} \left\{ \int_0^x dx' F_n \left(\frac{\sqrt{v'^2}}{v_{T_n}} \right) + \int_0^L dx' F_n \left(-\frac{\sqrt{v'^2}}{v_{T_n}} \right) \right\} \frac{1}{\sqrt{v'^2}} \exp \left\{ \frac{e\Phi(x')}{kT_e} \right\} H(v'^2), \quad (14)$$

$$f_i^-(x, v) = B \frac{n_0}{L} \int_x^L dx' \frac{1}{\sqrt{v'^2}} \exp \left\{ \frac{e\Phi(x')}{kT_e} \right\} H(v'^2) F_n \left(-\frac{\sqrt{v'^2}}{v_{T_n}} \right). \quad (15)$$

For the ion number density and the ion flux from Eqs. (14) and (15) we have

$$\begin{aligned} n_i(x) &= \int_0^\infty dv \{f_i^+ + f_i^-\} \\ &= 2B \frac{n_0}{L} \int_0^\infty dv \left\{ \int_0^L \frac{dx'}{\sqrt{v'^2}} F_n \left(-\frac{\sqrt{v'^2}}{v_{T_n}} \right) H(v'^2) \exp \left\{ \frac{e\Phi(x')}{kT_e} \right\} \right. \\ &\quad \left. + \int_0^x \frac{dx'}{\sqrt{v'^2}} \left[F_n \left(\frac{\sqrt{v'^2}}{v_{T_n}} \right) - F_n \left(-\frac{\sqrt{v'^2}}{v_{T_n}} \right) \right] H(v'^2) \exp \left\{ \frac{e\Phi(x')}{kT_e} \right\} \right\}, \end{aligned} \quad (16)$$

$$\begin{aligned} J_i(x) &= \int_0^\infty dv v \{f_i^+ - f_i^-\} \\ &= B \frac{n_0}{L} \int_0^\infty dv v \int_0^x \frac{dx'}{\sqrt{v'^2}} \exp \left\{ \frac{e\Phi(x')}{kT_e} \right\} H(v'^2) \left\{ F_n \left(\frac{\sqrt{v'^2}}{v_{T_n}} \right) + F_n \left(-\frac{\sqrt{v'^2}}{v_{T_n}} \right) \right\} \end{aligned} \quad (17)$$

In order to find the floating potential by comparing the ion and the electron fluxes onto the wall, we further analyze the expression of the ion flux $J_i(L)$ from Eq. (17) at $x = L$. For the Maxwellian source the auxiliary function (9) is

$$F_n \left(\frac{v}{v_{T_n}} \right) = \exp \left(-\frac{v^2}{2v_{T_n}^2} \right). \quad (18)$$

At this point we introduce the dimensionless quantities

$$u = \frac{v}{\sqrt{2}c_s}, \quad \frac{e\Phi(x)}{kT_e} \rightarrow \Phi(x), \quad \frac{x}{L} \rightarrow x, \quad n = \frac{n_i}{n_0}, \quad j = \frac{J_i}{n_0 c_s}, \quad \tau = \frac{T_e}{T_n}, \quad c_s = \sqrt{\frac{kT_e}{m_i}}. \quad (19)$$

The expressions for the ion density and the ion flux in Eqs. (16) and (17) can be simplified to

$$\begin{aligned} n(x) &= 2B \int_0^\infty du \int_0^1 dx' \exp(\Phi(x')) \\ &\quad \times \frac{\exp(-\tau\{u^2 - \Phi(x') + \Phi(x)\})}{\sqrt{u^2 - \Phi(x') + \Phi(x)}} H(u^2 - \Phi(x') + \Phi(x)), \end{aligned} \quad (20)$$

$$\begin{aligned} j(L) &= 2\sqrt{2}B \int_0^\infty du u \int_0^1 dx' \exp(\Phi(x')) \\ &\quad \times \frac{\exp(-\tau\{u^2 - \Phi(x') + \Phi(x)\})}{\sqrt{u^2 - \Phi(x') + \Phi(x)}} H(u^2 - \Phi(x') + \Phi(x)). \end{aligned} \quad (21)$$

The integral over x' in Eq. (20) can be split into two parts

$$\int_0^1 dx'(\dots) = \int_0^x dx'(\dots) + \int_x^1 dx'(\dots). \quad (22)$$

In the first interval $(0, x)$ of the integration we see that $\Phi(x') - \Phi(x) \geq 0$ holds, and in the second $\Phi(x') - \Phi(x) \leq 0$. This allows us to use the cut-off property of the H -function and finally we find

$$n(x) = B \int_0^1 dx' \exp[\Phi(x')] \exp \left[\frac{\tau}{2} \{\Phi(x') - \Phi(x)\} \right] K_0 \left\{ \frac{\tau}{2} |\Phi(x') - \Phi(x)| \right\}, \quad (23)$$

$$j(1) = \sqrt{\frac{2\pi}{\tau}} B \int_0^1 dx' \exp[\Phi(x')] . \quad (24)$$

In obtaining Eq. (23), the relation

$$2 \int_0^\infty \frac{\exp(-\tau x^2)}{\sqrt{x^2 + a^2}} = \exp\left(\frac{\tau}{2} a^2\right) K_0\left(\frac{\tau a^2}{2}\right) \quad (25)$$

was also used. Here $K_0(z)$ is the modified Bessel function of zero order. Eq. (23) coincides with the expression for the ion density used in [6] and [7]. In the limit of the cold source, $T_n \rightarrow 0$ where the auxiliary function reads $F_n(v/v_{T_n}) = \sqrt{2\pi} v_{T_n} \delta(v)$, ($\delta(z)$ is the Dirac δ -function) we find the expression for the ion density

$$n(x) = \frac{1}{\sqrt{2}} \int_0^x \frac{dx'}{\lambda_i} \frac{\exp[\Phi(x')]}{\sqrt{\Phi(x') - \Phi(x)}} \quad (26)$$

discussed previously in detail in [9, 10]. In Eq. (26) λ_i is defined by Eq. (12). In notation (19) Poisson's Eq. (3) acquires the form

$$\begin{aligned} B \int_0^1 dx' \exp[\Phi(x') - \Phi(x)] \exp\left[\frac{\tau}{2}\{\Phi(x') - \Phi(x)\}\right] K_0\left\{\frac{\tau}{2}|\Phi(x') - \Phi(x)|\right\} \\ = 1 - \varepsilon^2 \exp(-\Phi) \frac{d^2\Phi}{dx^2} \end{aligned} \quad (27)$$

where $\varepsilon = \lambda_D/L$ is the arbitrary parameter and $\lambda_D = \sqrt{\epsilon_0 k T_e / e^2 n_0}$ is the electron Debye length. Eq. (27) describes the potential profile for the arbitrary temperature of the source. When considering $\vartheta = 1/\Theta$ the main equation of the problem becomes

$$\begin{aligned} \frac{1}{B} = \frac{1}{1 - \exp(-\Phi) \varepsilon^2 \frac{d^2\Phi}{dx^2}} \\ \times \int_0^1 dx' \exp\left[\left(\vartheta + \frac{\tau}{2}\right)\Phi(x') - \left(1 + \frac{\tau}{2}\right)\Phi(x)\right] K_0\left\{\frac{\tau}{2}|\Phi(x') - \Phi(x)|\right\} . \end{aligned} \quad (28)$$

With explicit source distribution and ϑ the non-dimensional form of ion VDF is

$$f_i(\Phi(x), v) = B \int_0^1 dx' \exp(\vartheta\Phi') \frac{\exp[-(v^2 - (\Phi' - \Phi))/T_n]}{\sqrt{v^2 - (\Phi' - \Phi)}} . \quad (29)$$

Please note that we replaced the original H&T notation of the ionization profile $\exp(\gamma e\Phi/kT_e)$ with $\exp(\vartheta e\Phi/kT_e)$ for the reason that coauthors of the present work use “ γ ” symbol as exclusive denotation for the “polytropic” coefficient (see e.g., Ref. [11]). Using Eq. (8) and Eq. (24) for finding the floating potential of the wall we obtain the relation

$$\exp(\Phi_w) = 2\pi \sqrt{\frac{m_e}{m_i}} \sqrt{T_n} B \int_0^1 dx' \exp[\Phi(x')] . \quad (30)$$

3 ANALYTIC-NUMERICAL METHOD

Equation (28) is a Fredholm type integro-differential equation with a singular kernel and nonlinear function related to Poisson Eq. (3). Solution function $\Phi(x)$ is known to be smooth and monotonous and also to have endpoint singularity when $\varepsilon = 0$. Additionally, Eq. (28) contains unknown constant B that represents “eigenvalue” of the system. In collocation methods the singular behavior at the boundaries of the interval $[0, 1]$ can be taken into account by using non-uniform grids with increasing density when approaching singularity. For N collocation points we introduce the following node positions

$$x_i = \left[1 - [1 - i/(N - 1)]^{\lambda_2}\right]^{\lambda_1}, \quad i = 0, 1, \dots, N - 1, \quad (31)$$

where λ_1 and λ_2 control the density at each boundary. Rearranging Eq. (28) into a form suitable for an iterative procedure and discretizing it into subintervals we obtain

$$\begin{aligned} \exp \left[\left(1 + \frac{1}{2T_n}\right)V_k \right] = & \frac{B}{1 - \exp(-\Phi)\varepsilon^2 \frac{d^2\Phi(x)}{dx^2}} \\ & \times \sum_{i=0}^{N-1} \int_{x_i}^{x_{i+1}} dx' \exp\left[\left(\vartheta + \frac{1}{2T_n}\right)V(x')\right] K_0 \left(\frac{1}{2T_n} |V(x') - V_k| \right). \end{aligned} \quad (32)$$

Each node value V_k is also a source for diagonal singularity in kernel $K_0(z)$ (a singularity as $x' \rightarrow x_k$). In practice, the computation on strongly graded grids may be unstable since the grid points may be located too close to each other near boundaries and the system of equations may become rapidly ill-conditioned with increasing λ_1 , λ_2 and N .

We refer to Ref. [8] for details. In this contribution we extend the domain of applicability of this technique to $\varepsilon = 0$ and $\vartheta = 0$. To overcome stability problems we introduce a mildly graded piecewise Lagrangian polynomial interpolation of order 2 and 3. Although such approximation is often considered to be too expensive for numerical computation, it possesses beautiful symmetry and with a modified (weighted) form is comparable in speed to other approximations. Additionally, we found that solution for $\vartheta = 0$ (flat ion-source profile) is surprisingly stiffer than for $\vartheta = 1$. This could be due to imbalance in $\exp(z)$ functions on both sides of Eq. (32). Shifting of the whole solution for $-V_0$ was required to speedup convergence as shown in Fig. 2 where we illustrate the diagnostic procedure of obtaining “saturated” solution. The staircase effect in Fig. 2(b) is just an illustration of a local convergence when shifting to the origin is not performed within dense intervals. Such behavior was not observed for $\vartheta = 1$. Fig. 2(a) shows that endpoint value Φ_s converges faster than B . An additional advantage of our program package is a feature of automatic checking of the convergence criterion for both Φ_s and B .

4 RESULTS

In Fig. 3 we show the results of a huge number of simulations performed with our program package. The novelty in the last version is that we have possibility to calculate the results with various ion source spatial distribution. In Fig. 3(a) we show the classical case of Kos et al. [8] while in Fig. 3(b) we show the results obtained for the purpose of present investigation.

In Fig. 4 we show quantitative results, i.e., comparison of the results obtained with “classical” ion source distribution as employed by B&J, S&E and Kos et al. with the result obtained in the current investigation (constant ion source).

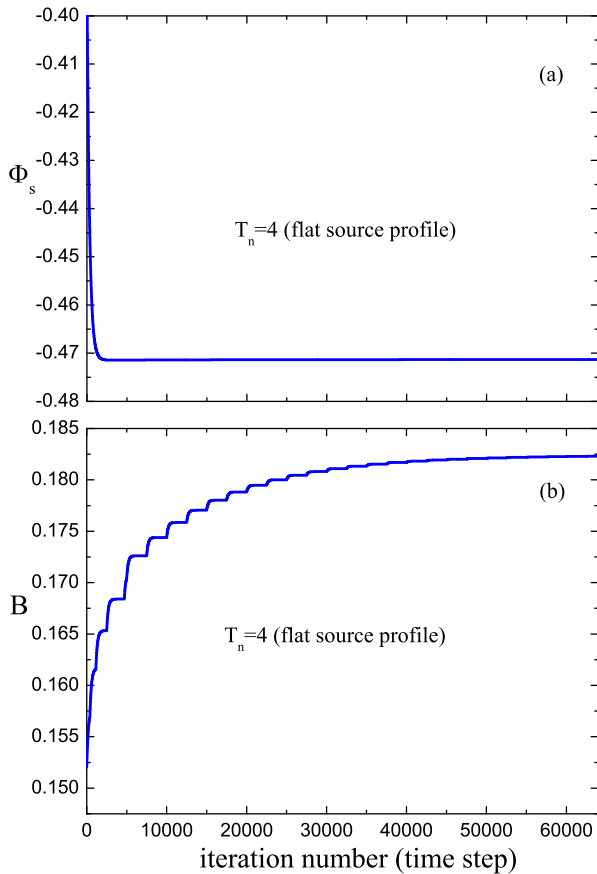


Figure 2: Convergence plots for $T_n = 4$ and flat source: (a) Boundary point Φ_s , and (b) eigenvalue B .

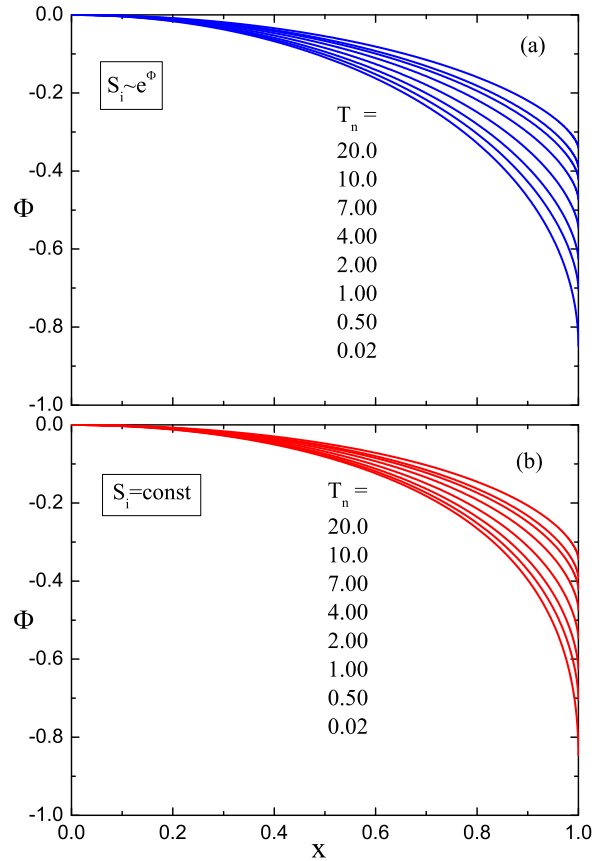


Figure 3: Comparison of potential profiles for (a) Boltzmannian ion source distribution and (b) Constant ion source distribution.

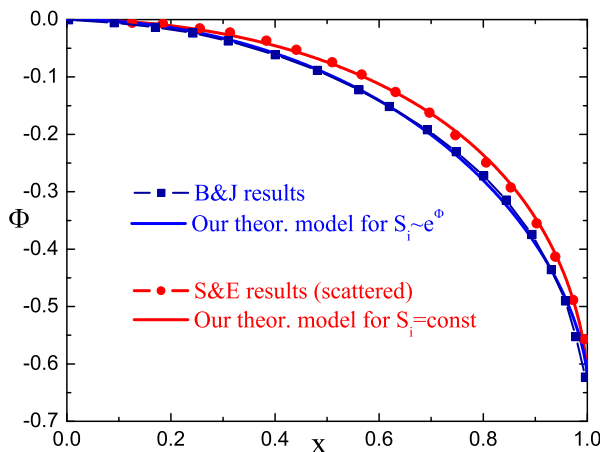


Figure 4: Comparison of B&J (blue scattered) with our analytic-numerical model (blue solid line) and S&E (red scattered) with our analytic-numerical method for flat ion-source.

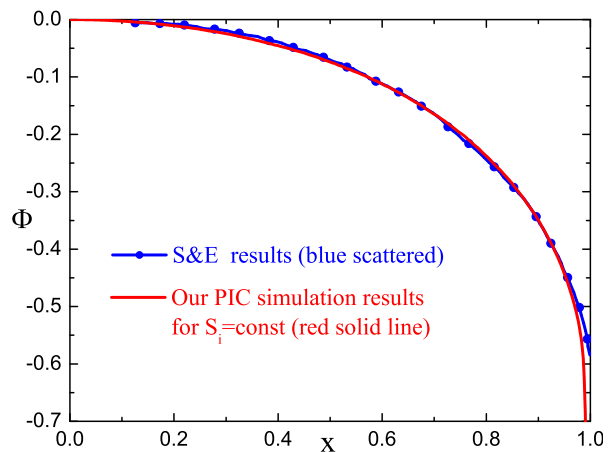


Figure 5: Comparison of S&E results (blue scattered) with our PIC simulation (red solid line)

In Fig. 5 we compare our results of a constant ion source with scanned results of S&E. It turns out that S&E in fact worked with the constant ion source and NOT with the source proportional to electron density. Fig. 6 shows the plasma potential at the point of the electric field singularity. The difference between the cases corresponding either of above sources is so small that it could not be seen within the drawing accuracy at all. This result is well aligned with the theoretical predictions of e.g., Caruso and Cavaliere [2].

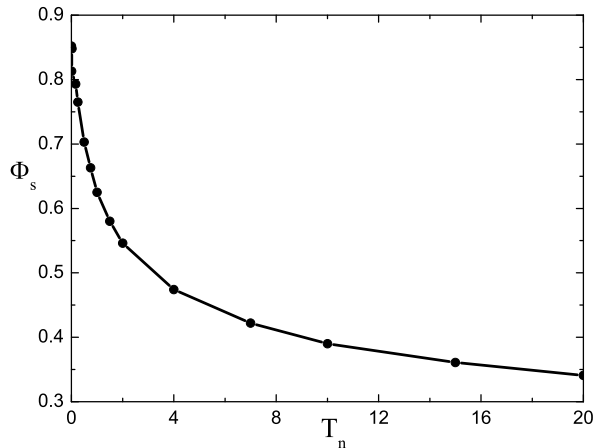


Figure 6: Boundary potential Φ_s dependency on the normalized ion-source temperature T_n .

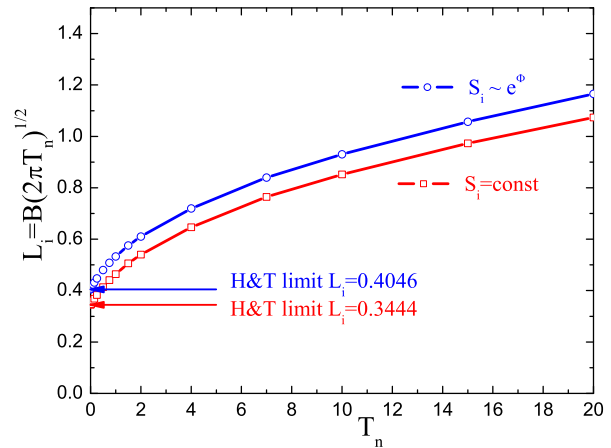


Figure 7: Ionization lengths of two alternative ionization mechanism as defined by H&T.

In Fig. 7 we show our *capital* result, i.e., comparison of the results obtained for the two alternative source profiles. While over several decades the results were known only for cold ion sources (we illustrate the cases of H&T as single points) our results extend to any ion-source (e.g., neutral) temperature.

5 DISCUSSION AND CONCLUSION

Our investigation covers a wide range of ion-source temperatures for $\vartheta = 0$. In fact this is the first investigation of the kind using the analytic-numerical method. (Other methods assume employment of PIC method (see e.g., Krek. et al. [12]).

Our main result is obtaining the ionization length for an arbitrary ion temperature (Fig. 7) and for arbitrary ionization profile strength. A particular case of flat ionization profile is elaborated in details and compared with “classical” B&J model, showing that the plasma-sheath boundary potential Φ_s is *invariant* on the particular ionization profile choice. The detailed profiles and the ionization lengths, on contrary, are *not* invariant on the particular potential profile choice. The dependence of the ionization length on the ion-source (neutral gas) temperature is investigated in detail for both flat and Boltzmann-distributed ionization sources.

In addition, this work also shows how to extend the results to finite (arbitrary) ε which will be considered in a forthcoming paper.

ACKNOWLEDGMENTS

This work was supported by the European Commission under (i) the Contract of Association between EURATOM and the Austrian Academy of Sciences and (ii) the Contract of Association between The European Atomic Energy Community (EURATOM) and the Ministry of Higher

Education, Science and Technology of the Republic of Slovenia No. FU06-CT-2007-00065, and by (iii) the Austrian Science Fund (FWF) under project P19333-N16. It was carried out within the framework of the European Fusion Development Agreement. The views and opinions expressed herein do not necessarily reflect those of the European Commission. Numerical calculations associated with this work were supported by the Austrian Ministry of Science and research (BMWf) as part of the UniInfrastrukturprogramm of the Forschungsplattform Scientific Computing at the Leopold-Franzens Universität (LFU) Innsbruck. The authors are indebted to K.-U. Riemann for his permanent advice and instructions on theoretical aspects. We are especially obliged to D. D. Tskhakaya Sr. for checking out the formula derivations and many valuable discussions on physical theoretical points.

REFERENCES

- [1] L. Tonks and I. Langmuir. A general theory of the plasma of an arc. *Phys. Rev.*, 34(6):876–922, Sep 1929.
- [2] A. Caruso and A. Cavaliere. The structure of the collisionless plasma-sheath transition. *Il Nuovo Cimento (1955-1965)*, 26(6):1389–1404, 1962.
- [3] E. R. Harrison and W. B. Thompson. The low pressure plane symmetric discharge. *Proceedings of the Physical Society*, 74(2):145–152, 1959.
- [4] S. A. Self. Exact solution of the collisionless plasma-sheath equation. *Physics of Fluids*, 6:1762, 1963.
- [5] A. Emmert, R. M. Wieland, A. T. Mense, and J. N. Davidson. Electric sheath and presheath in a collisionless, finite ion temperature plasma. *Physics of Fluids*, 23(4):803–812, 1980.
- [6] R. C. Bissell and P. C. Johnson. The solution of the plasma equation in plane parallel geometry with a Maxwellian source. *Physics of Fluids*, 30(2):779–786, 3 1987.
- [7] J. T. Scheuer and G. A. Emmert. Sheath and presheath in a collisionless plasma with a maxwellian source. *Physics of Fluids*, 31(12):3645–3648, 1988.
- [8] L. Kos, N. Jelić, S. Kuhn, and Jože Duhovnik. Extension of the Bissel-Johnson plasma-sheath model for application to fusion-relevant and general plasmas. *Physics of Plasmas*, 16(9), 9 2009. (to appear)
- [9] K.-U. Riemann. The Bohm criterion and sheath formation. *Journal of Physics D: Applied Physics*, 24(4):493–518, 1991.
- [10] K.-U. Riemann. Plasma-sheath transition in the kinetic Tonks-Langmuir model. *Physics of Plasmas*, 13(6):063508, 2006.
- [11] S. Kuhn, K.-U. Riemann, N. Jelić, D. D. Tskhakaya, Sr., D. Tskhakaya, Jr., and M. Stanojević. Link between fluid and kinetic parameters near the plasma boundary. *Physics of Plasmas*, 13(1):013503, 2006.
- [12] N. Jelić, J. Krek, S.t Kuhn, and J. Duhovnik. Particle-in-cell (PIC) simulations of the plasma-sheath boundary in finite- ϵ plasmas with warm ion source of constant temperature. *Physics of Plasmas*, 2009. (to be submitted).